

# X-ray photometry

M. J. Page<sup>★</sup>

*Mullard Space Science Laboratory, University College London, Holmbury St Mary, Dorking, Surrey RH5 6NT, UK*

Accepted 2015 June 18. Received 2015 June 18; in original form 2015 March 13

## ABSTRACT

I describe a method for synthesizing photometric passbands for use with current and future X-ray instruments. The method permits the standardization of X-ray passbands and thus X-ray photometry between different instruments and missions. The method is illustrated by synthesizing a passband in the *XMM–Newton* European Photon Imaging Camera pn which is similar to the *ROSAT* Position Sensitive Proportional Counter 0.5–2 keV band.

**Key words:** methods: data analysis – methods: observational – techniques: photometric – X-rays: general.

## 1 INTRODUCTION

Photometry, the measurement of source brightness in a given wavelength range, is one of the most fundamental techniques in astronomy. It is practised throughout the electromagnetic spectrum, and X-ray astronomy is no exception. In optical astronomy, photometric passbands have been standardized between observatories since the introduction of the Johnson and Morgan system (Johnson & Morgan 1953); see Bessel (2005) for a review. The benefits of a well-defined set of photometric X-ray bands have been recognized before (e.g. Grimm et al. 2009) but despite more than 50 years of X-ray astronomy, there is as yet no system of photometric passbands that applies to more than a single X-ray observatory. In this Letter, I will describe the concept of synthesized X-ray passbands that can be applied to existing and future X-ray astronomy instruments, and so permit the establishment of standard, multimission X-ray photometric passbands. As an example, I will show that the *ROSAT* Position Sensitive Proportional Counter (PSPC) 0.5–2 keV passband can be synthesized with the *XMM–Newton* European Photon Imaging Camera (EPIC)-pn camera, so that X-ray photometry gathered with *ROSAT* and *XMM–Newton* can be compared directly.

## 2 DEFINITIONS

I will adopt a definition of photometry as the measurement of source brightness through a well-defined passband relative to some standard reference. The standard reference could be an astronomical object such as the star Vega. Alternatively it could be a theoretical reference, such as the constant flux density spectrum used as a reference in the AB system (Oke 1965, 1974), provided that the throughput of the instrument performing the photometric measurements is sufficiently well calibrated. Almost all measurements of source brightness in X-ray astronomy may be considered to conform to such a definition: the curves of effective area against energy

commonly employed in X-ray astronomy represent well-defined passbands which have already been calibrated in physical units. However, X-ray photometry is disadvantaged with respect to e.g. optical photometry, is that each instrument on each X-ray observatory has a different effective area curve. To mitigate this problem, X-ray astronomers have developed tools such as PIMMS<sup>1</sup> (Mukai 1993) which allow a measurement with one instrument to be translated into a predicted count rate for a different instrument, given a model for the X-ray spectrum of the source. However, if the spectrum of the source is not known or is only poorly determined, then the predicted count rate will not be accurate.

In a photon counting detector, as usually employed in X-ray astronomy instrumentation, the count rate  $C$  can be related to the spectrum of a source and the effective area of the instrument as follows:

$$C = \int_{\nu_{\min}}^{\nu_{\max}} \frac{f_{\nu}(\nu)}{h\nu} A(\nu) d\nu, \quad (1)$$

where  $\nu$  is frequency,  $h$  is the Planck constant,  $f_{\nu}(\nu)$  is the flux per unit frequency interval of the source and  $A(\nu)$  is the effective area of the instrument. For an imaging system, it is assumed that  $A(\nu)$  is the overall effective area of the instrument and telescope combined. The limits  $\nu_{\min}$  and  $\nu_{\max}$  are the minimum and maximum frequencies at which  $A(\nu)$  is significant.

If we define

$$K = \max \left( \frac{A(\nu)}{h\nu} \right)$$

and

$$R(\nu) = \frac{A(\nu)}{Kh\nu},$$

so that  $R(\nu)$  is the normalized response curve of the system, then

$$\frac{C}{K} = \int_{\nu_{\min}}^{\nu_{\max}} f_{\nu}(\nu) R(\nu) d\nu. \quad (2)$$

<sup>★</sup> E-mail: [m.page@ucl.ac.uk](mailto:m.page@ucl.ac.uk)

<sup>1</sup> <https://heasarc.gsfc.nasa.gov/docs/software/tools/pimms.html>

The fundamental quantity measured in astronomical photometry is the quantity on the right-hand side of equation (2), the integral over the passband of the flux of the source multiplied by the response of the system. The quantity on the left-hand side of equation (2) is the measurement itself, the count rate divided by the peak effective area of the system. In optical astronomy, the measurement is usually expressed as a magnitude  $m$ ,

$$m = -2.5 \log_{10} \int_{\nu_{\min}}^{\nu_{\max}} f_{\nu}(\nu) R(\nu) d\nu + z,$$

where  $z$  is the zero-point, defined such that a reference standard has zero magnitude (e.g. Cousins & Jones 1976). A Vega-based magnitude system would not be appropriate in the X-ray regime, because Vega has yet to be convincingly detected as an X-ray source (Pease, Drake & Kashyap 2006; Ayres 2008), but the AB magnitude system would be well suited to X-ray astronomy. None the less, the adoption of magnitudes as a convenient unit is not necessary for the establishment of a system of photometric passbands in X-ray astronomy. What is essential is the ability to perform the measurement described by equation (2) with different instruments on different observatories with similar response functions, or passbands,  $R(\nu)$ .

### 3 SYNTHESIZING PHOTOMETRIC PASSBANDS

The synthesis of a passband is only possible for instruments which discriminate the energies of the incoming photons. In X-ray astronomy, data are usually telemetered to Earth as ‘event lists’, in which the individual photons are listed with their properties such as arrival time, position on the detector and energy channel. The energy resolution of non-dispersive Charge-Coupled Device (CCD) based X-ray instruments is limited, usually  $10 < R < 50$  (e.g. Strüder et al. 2001; Turner et al. 2001), so the relationship between energy channel and (real) photon energy is described by the redistribution matrix. The redistribution matrix contains, for a sequence of discrete energy ranges, the probability of a photon within that energy range being recorded in each of the energy channels. I will refer to the product of the redistribution matrix and the effective area as a function of energy (i.e. for each discrete energy range, the channel probability distribution multiplied by the effective area in that energy range) as the response matrix.<sup>2</sup> For each energy channel  $i$ , the response matrix contains the effective area for that channel as a function of energy, and therefore frequency  $A_i(\nu)$ .

X-ray astronomers choose passbands for their instruments by selecting ranges of energy channels which correspond to their desired energy ranges; the *Chandra* Advanced Camera for Imaging and Spectroscopy (ACIS) bands advocated by Grimm et al. (2009), and the bands chosen for the 2XMM catalogues (Watson et al. 2009) are examples of this approach, and I will refer to these bands as natural instrumental passbands. For natural passbands, the count rate in the band  $C$  is related to the count rates in the individual energy channels  $C_i$  by

$$C = \sum_{i_{\min}}^{i_{\max}} C_i,$$

<sup>2</sup> It should however be noted that, somewhat confusingly, it is quite common in X-ray astronomy to use the term ‘response matrix’ interchangeably with ‘redistribution matrix’.

where  $i_{\min}$  and  $i_{\max}$  are the minimum and maximum channels of the passband. The effective area of the band  $A(\nu)$  is related to the effective areas  $A_i(\nu)$  of the individual channels by

$$A(\nu) = \sum_{i_{\min}}^{i_{\max}} A_i(\nu).$$

While natural passbands can be chosen to cover similar energy ranges with different instruments on different missions, there is little scope in this approach to control (and thus standardize) the shapes  $R(\nu)$  of the passbands.

To synthesize a passband, it must be possible to control the shape as well as the energy range. This can be accomplished by assigning weights  $w_i$  to the channels that form the band when calculating the count rate within the band. Thus for a synthesized band:

$$C = \sum_{i_{\min}}^{i_{\max}} w_i C_i$$

and

$$A(\nu) = \sum_{i_{\min}}^{i_{\max}} w_i A_i(\nu).$$

The weights can be chosen so that the synthesized band has a response  $R(\nu)$  as close as possible to the response desired. The weights  $w_i$  therefore act as a synthetic filter, controlling the shape of the passband. The capability to compose and apply the synthetic filter after the data have been taken is a distinct advantage of X-ray instrumentation compared to that employed for photometry at longer wavelengths.

### 4 PRACTICAL CONSIDERATIONS

In order to synthesize a passband with an instrument, the instrument must be sensitive over a similar or larger frequency range than that covered by the passband. The degree to which the shape of a passband can be controlled by the choice of the weights  $w_i$  depends on the width of the channel distribution at a given energy in the response matrix (i.e. the energy resolution of the instrument) and to a lesser degree on the shape of this distribution. The introduction of the weights  $w_i$  implies a reduction in the signal to noise of the count rate with respect to that in a natural passband. In general, X-ray instruments have improved in both spectral resolution and collecting area with time, and this trend is expected to continue with the future European Space Agency mission *Athena* (Nandra et al. 2013). Thus, it is more practical to use present-day or future instruments to synthesize the natural bands of earlier X-ray astronomy instruments than the other way round.

In general, the more closely the response curves  $R(\nu)$  of two passbands match, the more similar the photometry will be between them. Therefore the best photometric performance from a synthesized band will be obtained by choosing the weights  $w_i$  to match as closely as possible the desired  $R(\nu)$ . On the other hand, the smoother and more uniform the  $w_i$ , the higher the signal to noise will be. Therefore, in choosing the weights  $w_i$ , there might be some trade-off between obtaining the desired shape  $R(\nu)$  and maximizing the signal-to-noise ratio, particularly if the best match to  $R(\nu)$  corresponds to large fluctuations in  $w_i$  between adjacent channels.

Another consideration is that the count rate in a synthesized band will no longer be Poisson distributed as it is in natural bands; instead it will be distributed as the sum of the weighted Poisson distributions, and error analysis is more involved. However, the subtraction

of background also causes the count rates of sources to deviate from Poisson statistics, and this is routinely performed in X-ray astronomy already, so the importance of this consideration should not be exaggerated. None the less, the reduction of signal to noise and the increased complexity of error analysis are disadvantages associated with synthesized passbands, to be traded off against the advantages of standardizing the passbands between missions.

## 5 AN EXAMPLE SYNTHESIZED PASSBAND

As an example, I will now show that the 0.5–2 keV band of the *ROSAT* PSPC can be synthesized with the *XMM-Newton* EPIC-pn instrument (Strüder et al. 2001). To date the only imaging all-sky survey carried out in X-rays used the *ROSAT* PSPC, so this instrument has provided photometric measurements of a large body of X-ray sources (Voges et al. 1999). Many of these sources have been observed subsequently with *XMM-Newton*. It would be useful to be able to compare directly the photometric measurements from *ROSAT* and *XMM-Newton*, for example to study the long-term variability of X-ray sources. Following the logic of Section 4, it is more practical to synthesize the *ROSAT* PSPC passband with the *XMM-Newton* EPIC pn than the other way around, because EPIC pn has better energy resolution, and a larger effective area than the PSPC.

The *ROSAT* PSPC 0.5–2 keV band is formed from PSPC energy channels<sup>3</sup> 52–201. The normalized response  $R(\nu)$  of this band is shown as the grey curve in Fig. 1. The distribution of weights  $w_i$  to be applied to the EPIC-pn channels was obtained by iteratively adjusting the weights so as to minimize the sum of the squares of the difference between the PSPC and synthesized response  $R(\nu)$  at each point of the  $R(\nu)$  curve over the frequency range of the synthetic band, i.e. a least-squared fit. No smoothing criteria were applied during the fitting of the weights. Fig. 2 shows the channel weights  $w_i$  corresponding to the synthesized passband. The distribution of  $w_i$  is quite smooth with fluctuations between adjacent channels rarely exceeding 2 per cent, so smoothing the  $w_i$  would have little impact on the signal-to-noise ratio of photometry through the synthesized band. The synthesized  $R(\nu)$  is shown as the black, dashed curve in Fig. 1. The match between the *ROSAT* PSPC and EPIC-pn synthesized bands is good, with  $R(\nu)$  differing by less than 0.01 over most of the band, and by no more than 0.05 at any point. However, the weak tail in the synthesized passband which stretches to higher frequency is irreducible, because it corresponds to the low-energy tail<sup>4</sup> of the CCD response.

To investigate the performance of the synthesized band in reproducing PSPC photometry, I have simulated a number of spectral models and folded them through the responses of the PSPC, EPIC-pn and the synthesized 0.5–2 keV band using *XSPEC11* (Arnaud 1996). For the normal EPIC-pn 0.5–2 keV response, I simply selected the pn channels that have nominal energies within the range 0.5–2 keV. The spectral models were chosen to span the range of spectral shapes typically exhibited by sources in the 0.5–2 keV band, and comprise power laws, with photon index  $\Gamma = 1, 2$  and 3, a power law with  $\Gamma = 2$ , absorbed by cold gas with a column density of  $N_{\text{H}} = 10^{22} \text{ cm}^{-2}$ , optically thin thermal plasmas (mekal in *XSPEC*) with  $kT = 0.3, 0.7$  and 1.5 keV and a blackbody with  $kT = 0.3$  keV.

<sup>3</sup> These are usually called pulse-height invariant or PI channels, because they correspond to the pulse height of an event after it has been calibrated for temporal and spatial gain variations on to a standard energy scale.

<sup>4</sup> i.e. redistribution of photons of a given energy to channels of lower energy.

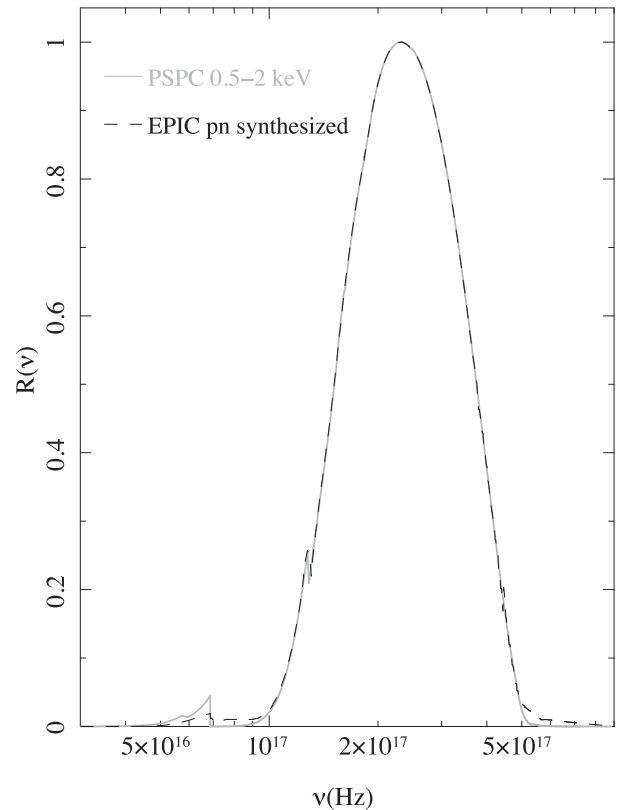


**Figure 1.** Passband of the *ROSAT* PSPC 0.5–2 keV band (solid curve) and an *XMM-Newton* EPIC-pn passband (dashed curve) which has been synthesized to have approximately the same shape.

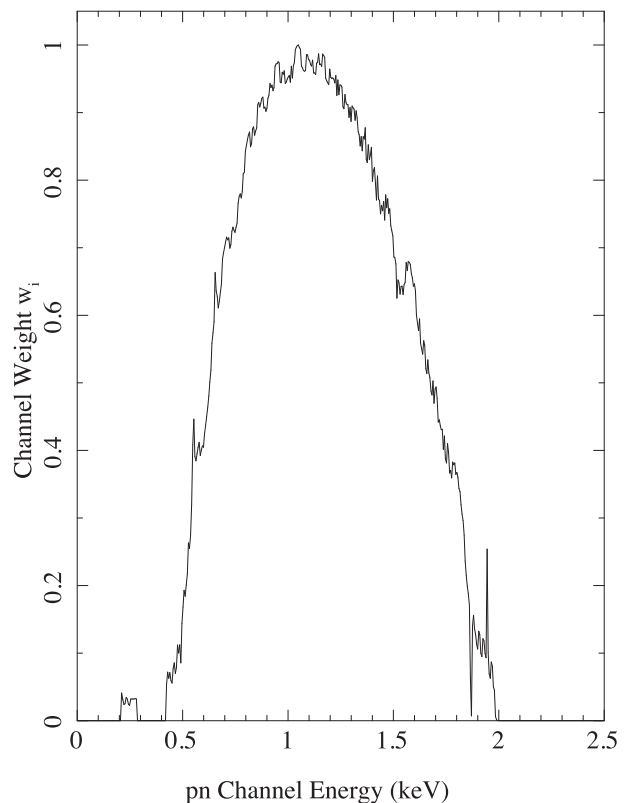


**Figure 2.** Weighting function applied to the EPIC-pn channels to produce the synthesized band shown in Fig. 1

**Table 1.** Simulated 0.5–2 keV photometry in the PSPC, EPIC-pn and the synthesized PSPC band for a number of spectral models. The second, third and fourth columns give the 0.5–2 keV flux that would be observed if the given spectrum is observed using the PSPC, EPIC-pn and synthesized PSPC passband, respectively, and the count rate is translated to a flux using a standard ECF. In all cases, the spectral model was normalized such that the true 0.5–2 keV flux is  $1.00 \times 10^{-14}$  erg cm $^{-2}$  s $^{-1}$ . The last two columns give the ratios of the flux that would be observed with EPIC-pn and the synthesized band, respectively, to the flux that would be observed with the PSPC.

Model	Simulated flux ( $10^{-14}$ erg cm $^{-2}$ s $^{-1}$ )			EPIC-pn / PSPC	Synthesized / PSPC
	PSPC	EPIC-pn	Synthesized		
Power law $\Gamma = 1$	0.96	0.96	0.96	1.00	1.00
Power law $\Gamma = 2$	1.02	1.02	1.02	1.00	1.00
Power law $\Gamma = 3$	1.04	1.04	1.03	1.00	0.99
Power law $\Gamma = 2$ , $N_{\text{H}} = 10^{22}$ cm $^{-2}$	0.68	0.84	0.71	1.25	1.04
Mekal $kT = 0.3$ keV	1.11	1.11	1.11	1.00	0.99
Mekal $kT = 0.7$ keV	1.32	1.12	1.31	0.85	0.99
Mekal $kT = 1.5$ keV	1.16	1.03	1.15	0.89	0.99
Blackbody $kT = 0.3$ keV	1.09	1.01	1.08	0.93	0.99

Each of the spectral models was normalized so as to have the same true 0.5–2 keV flux of  $10^{-14}$  erg cm $^{-2}$  s $^{-1}$ , and the count rates were simulated with zero statistical error, so that any differences in the photometry from the three passbands are systematic differences related to the shapes of the passbands.

In X-ray astronomy, photometry is normally derived from imaging surveys by measuring the count rate in a given band, and dividing this by an ‘energy conversion factor’ (ECF) which is specific to the instrument and band to obtain a flux in physical units. We have followed this process in simulating the photometry that would be obtained through the different passbands. The ECF itself is typically derived by folding a simulated source of known flux and spectral shape through the response of the instrument following the same procedure as we are employing to obtain the count rates for our simulated sources. To generate ECFs for the three passbands, we adopt the spectral model used for the 3XMM catalogue, a power law of photon index  $\Gamma = 1.7$  absorbed by cold gas with a column density  $N_{\text{H}} = 3 \times 10^{20}$  cm $^{-2}$  (Rosen et al. 2015). The ECFs for the PSPC, EPIC-pn and the synthesized band are  $7.65 \times 10^{10}$ ,  $6.67 \times 10^{11}$  and  $4.75 \times 10^{11}$  erg s $^{-1}$  cm $^2$ , respectively.

The results of the simulated photometry are given in Table 1. It can be seen that the flux derived from the PSPC differs significantly for several spectral models from the flux derived from photometry in the natural EPIC-pn 0.5–2 keV band. In the worst case of the heavily absorbed spectrum, the flux differs by 25 per cent. In contrast, the flux derived from the synthesized band differs from the PSPC flux by less than 1 per cent for all spectral models except for the strongly absorbed spectrum. In that case the difference is only 4 per cent, and is due to the weak tail towards higher energy in the synthesized response, where the absorbed spectrum is rising rapidly.

## 6 CONCLUSIONS

I have outlined a method for synthesizing photometric passbands in X-ray astronomy. It offers the potential to standardize photometry from different X-ray astronomy instruments and missions. I have limited this Letter to a conceptual description of the approach, and

provided an example to illustrate how it might be used. Widespread, practical application of the method will require considerably more work. Software tools will be required to optimize the shapes of the synthetic filters  $w_i$  used to shape the passbands, and software tools will be needed to compute photometry for real astronomical sources in the synthetic passbands. Not least, for this method to facilitate the large-scale provision of photometry in standardized X-ray passbands, there will need to be concordance within the X-ray astronomy community, at least amongst the curators of archives and the constructors of astronomical catalogues, as to what to choose as the minimum set of standard passbands.

## ACKNOWLEDGEMENTS

I thank Mark Cropper and Francisco Carrera for useful discussion.

## REFERENCES

- Arnaud K. A., 1996, in Jacoby G., Barnes J., eds, ASP Conf. Ser. Vol. 101, Astronomical Data Analysis Software and Systems V. Astron. Soc. Pac., San Francisco, p. 17
- Ayres T. R., 2008, *AJ*, 136, 1810
- Bessel M. S., 2005, *ARA&A*, 43, 293
- Cousins A. W. J., Jones D. H. P., 1976, *Mem. R. Astron. Soc.*, 81, 1
- Grimm H.-J., McDowell J., Fabbiano G., Elvis M., 2009, *ApJ*, 690, 128
- Johnson H. L., Morgan W. W., 1953, *ApJ*, 117, 313
- Mukai K., 1993, *Legacy*, 3, 21
- Nandra K. et al., 2013, preprint ([arXiv:1306.2307](https://arxiv.org/abs/1306.2307))
- Oke J. B., 1965, *ARA&A*, 3, 23
- Oke J. B., 1974, *ApJS*, 27, 21
- Pease D. O., Drake J. J., Kashyap V. L., 2006, *ApJ*, 636, 426
- Rosen S. R. et al., 2015, *A&A*, preprint ([arXiv:1504.07051](https://arxiv.org/abs/1504.07051))
- Strüder L. et al., 2001, *A&A*, 365, L18
- Turner M. J. L. et al., 2001, *A&A*, 365, L27
- Voges W. et al., 1999, *A&A*, 349, 389
- Watson M. G. et al., 2009, *A&A*, 493, 339

This paper has been typeset from a  $\text{\TeX}/\text{\LaTeX}$  file prepared by the author.